JOURNAL OF GEOPHYSICAL RESEARCH: OCEANS, VOL. 118, 410–421, doi:10.1029/2012JC008291, 2013

Source and formation of the upper halocline of the Arctic Ocean

Leif G. Anderson,[1] Per S. Andersson,[2] Göran Björk,[3] E. Peter Jones,[4]
Sara Jutterström,[5] and Iréne Wåhlström[1]

Received 18 June 2012; revised 7 November 2012; accepted 9 November 2012; published 31 January 2013.

[1] The upper halocline of the Arctic Ocean has a distinct chemical signature with high nutrient concentrations as well as low oxygen and pH values. This signature is formed in the Chukchi and East Siberian seas, by a combination of mineralization of organic matter and release of decay products to the sea ice brine enriched bottom water. Salinity and total alkalinity data show that the fraction of sea ice brine in the nutrient-enriched upper halocline water in the central Arctic Ocean is up to 4%. In the East Siberian Sea the bottom waters with exceptional high nutrient concentration and low pH have typically between 5 and 10% of sea ice brine as computed from salinity and oxygen-18 values. On the continental slope, over bottom depths of 150–200 m, the brine contribution was 6% at the nutrient maximum depth (50–100 m). At the same location as well as over the deeper basin the silicate maximum was found over a wider salinity range than traditionally found in the Canada Basin, in agreement with earlier observations east of the Chukchi Plateau. A detailed evaluation of the chemical and the temperature-salinity properties suggests at least two different areas for the formation of the nutrient-rich halocline within the East Siberian Sea. This has not been observed before 2004 and it could be a sign of a changing marine climate in the East Siberian Sea, caused by more open water in the summer season followed by more sea ice formation and brine production in the fall/winter.

Citation: Anderson, L. G., P. S. Andersson, G. Björk, E. Peter Jones, S. Jutterström, and I. Wåhlström (2013), Source and formation of the upper halocline of the Arctic Ocean, *J. Geophys. Res. Oceans*, *118*, 410–421, doi:10.1029/2012JC008291.

1. Introduction

[2] The Arctic Ocean consists of several water masses distributed from the surface to the bottom, each with a general circulation pattern [e.g., *Rudels et al*., 1994]. The surface water of the central Arctic Ocean has low salinity from sea ice melt and river runoff, where the latter is most pronounced in the Canadian Basin. Furthermore, the surface mixed layer has a seasonal signature with low salinity in the summer as a result of melting sea ice. During the fall and winter sea ice is produced and a winter surface layer of higher salinity is formed [e.g., *Rudels et al*., 1996]. Within the surface layer a large gyre typically exists in the Canada Basin, the Beaufort Gyre. Large quantities of fresh water can be trapped in this gyre [e.g., *McPhee et al*., 2009], with the dimension as well as its content of freshwater determined by the atmospheric pressure field [*Proshutinsky et al*., 2002; *Serreze et al*., 2006; *Houssais et al*., 2007; *Proshutinsky et al*., 2009; *Jahn et al*., 2010; *Timmermans et al*., 2011]. Below the surface layer there is a halocline that historically has been divided into the upper and lower haloclines [*Jones and Anderson*, 1986], where the former has a Pacific origin and the latter an Atlantic origin. The upper halocline (UH) is mainly confined to the Canadian Basin, and is identified by its maximum in nutrient concentration [e.g., *Kinney et al*., 1970; *Jones and Anderson*, 1986]. The horizontal extent of the UH varies over the years and was in 1981 observed over the North Pole during the LOREX ice camp study [*Moore et al*., 1983], while in 1991 it was absent at this location [*Anderson et al*., 1994]. Below the halocline is the Atlantic Layer with cyclonic circulation around the Arctic Ocean along the continental margins and the ridges [*Rudels et al*., 1994]. Below the Atlantic Layer are the deep and bottom waters that have little direct contact with the surrounding oceans and thus are of a relatively high age, 50 to several hundred years [e.g., *Schlosser et al*., 1997; *Tanhua et al*., 2009].

[3] The Arctic Ocean is impacted by environmental change in several ways with the decrease in summer sea ice coverage being the most pronounced. This change impacts the marine environment both physically as well as biochemically. Less summer sea ice coverage in the shelf sea opens for more light that promotes primary productivity [e.g., *Arrigo et al*., 2008, *Pabi et al*., 2008] making it possible to better utilize available nutrients, which will increase the sediment load to these shallow sediments. With a larger area of open water in the fall there is a potential for more sea ice production, as the heat loss

[1]Department of Chemistry and Molecular Biology, University of Gothenburg, Sweden.
[2]Laboratory for Isotope Geology, Swedish Museum of Natural History, Sweden.
[3]Department of Earth Sciences, University of Gothenburg, Sweden.
[4]Bedford Institute of Oceanography, Dartmouth, Canada.
[5]IVL Swedish Environmental Research Institute, Sweden.

Corresponding author: L. G. Anderson, Department of Chemistry and Molecular Biology, University of Gothenburg, SE-412 96, Gothenburg, Sweden. (leifand@chem.gu.se)

2169-9275/13/2012JC008291

is higher in open water compared to ice covered waters. Consequently there is also a potential for more brine to be produced that can add to the salinity of the bottom water on the shelves.

[4] The high salinity shelf bottom waters with their elevated nutrient concentrations are a source of the UH [e.g., *Jones and Anderson*, 1986]. Because the main source of the nutrients is mineralization of organic matter, the waters also have high partial pressure of carbon dioxide (pCO_2) and low pH, making them corrosive for calcium carbonates [e.g., *Anderson et al*., 2010]. However, when the central Arctic Ocean was ice covered in the summer as well, the UH was confined to a depth well below 50 m and thus no primary production occurred in this layer. The melting of the sea ice coverage has resulted in a decrease of the surface water salinity and thus an increase of the salt-stratification below the seasonal mixed layer. The freshening of the surface layer leads to a lowering of the calcium ion concentration and thus also the calcium carbonate saturation, in some regions even to a level where the surface water is undersaturated [*Yamamoto-Kawai et al*., 2011]. On the other hand, the increase in stratification has also hampered the vertical mixing and thus the input of low pH water from the UH to the surface layer in the winter.

[5] We show that the formation of nutrient-rich water found on the shelf and at the shelf slope has more variable salinity properties than what has been obtained from historical data. We also show that brine from sea ice production is an important property of the UH and hypothesize that less sea ice coverage over the East Siberian Shelf in summer sets the conditions for the more variable salinity of the UH. Furthermore, with the expansion of the salinity range of the UH to lower values, this water gets closer to the surface and thus possibly impacting the surface waters of the central Arctic Ocean, e.g., by increasing the nutrient supply.

2. Methods

2.1. Sampling

[6] The shelf data were collected during the International Siberian Shelf Study in 2008 (ISSS-08) from the Russian vessel *Yacob Smirnitskyi* in September 2008, while the central Arctic Ocean data were collected during the Beringia transpolar cruise on board the Swedish icebreaker *Oden* from 21 August to 20 September 2005. The station locations of the cruises are shown in Figure 1. Hydrographic casts for both cruises were performed by a rosette system with a Sea-bird 9/11 Conductivity, Temperature, Depth (CTD) sensor and water sample analysis for both cruises included dissolved oxygen, nutrients, total dissolved inorganic carbon (DIC), total alkalinity (TA), and pH.

2.2. Analyses

[7] The nutrients (phosphate, nitrate, nitrite, and silicate) collected during the ISSS-08 cruise were determined using an automatic spectrophotometric system (SmartChem from Westco). The samples were filtered before being analyzed and evaluated by a 6 to 8 points calibration curve, precision being ~1%. During the Beringia 2005 cruise they were determined using an auto-analyzer according to the World Ocean Circulation Experiment (WOCE) protocol [*Gordon et al*., 1993], on unfiltered samples with a precision ~1%. Oxygen was determined during both cruises using an automatic Winkler titration system, precision ~1 μmol kg^{-1}. DIC was determined by a coulometric titration method based on *Johnson et al*. [1987], having a precision of ~2 μmol kg^{-1}, with the accuracy set by calibration against certified reference materials, supplied by A. Dickson, Scripps Institution of Oceanography (USA). TA was determined by potentiometric titration, precision ~2 μmol kg^{-1}, [*Haraldsson et al*., 1997], with the accuracy set the same way as for DIC. pH was determined by spectrophotometric detection of pH [*Clayton and Byrne*, 1993; *Lee and Millero*, 1995], having a precision of ~0.003 pH units and the accuracy set by the equilibrium constants of the indicator. The values presented are on the total scale and are normalized to a temperature of 15 °C and atmospheric pressure.

[8] The stable oxygen isotopic compositions were determined using a Finnigan Delta V mass spectrometer, at Stockholm University, Department of Geological Sciences, applying the Thermal Conversion Elemental Analyzer (TC/EA). Results are given as per mil deviations from the standard

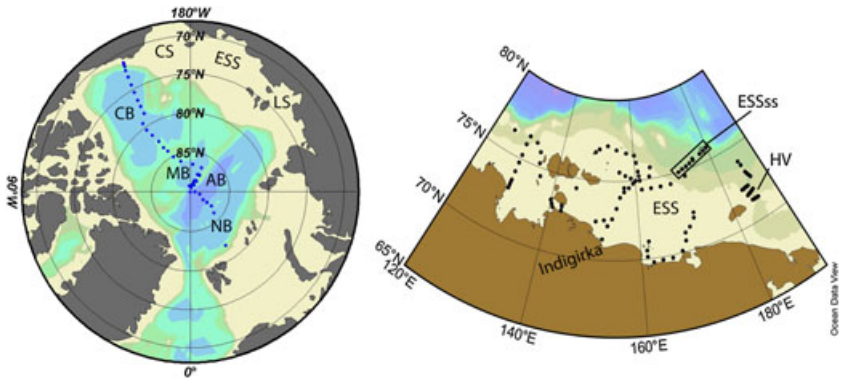

Figure 1. Location of the stations occupied during the Beringia 2005 cruise (left) and ISSS-08 cruise (right). Abbreviations are; CB - Canadian Basin, MB - Makarov Basin, AB - Amundsen Basin, NB - Nansen Basin, CS - Chukchi Sea, ESS - East Siberian Sea, LS - Laptev Sea, ESSss - East Siberian Sea shelf slope, and HV - Herald Valley. Figure drawn by Ocean Data View [*Schlitzer*, 2011].

(Vienna-SMOW) and denoted $\delta^{18}O$, where R is the ratio of $^{18}O/^{16}O$:

$$\delta^{18}O(‰) = \left(R_{\text{sample}}/R_{\text{standard}} - 1\right) \times 10^3. \quad (1)$$

[9] The overall measurement precision for $\delta^{18}O$ analysis is estimated to ±0.1‰ or smaller.

[10] The bottle data from the Beringia cruise is archived at the Clivar and Carbon Hydrographic Data Office (http://whpo.ucsd.edu/index.html) and the data from the ISSS-08 cruise (except $\delta^{18}O$) are archived at the PANGEA information system under the European Project on Ocean Acidification (EPOCA). The $\delta^{18}O$ data are archived at the GEOTRACES data repository at British Oceanography Data Center (http://www.bodc.ac.uk/geotraces/).

2.3. Source Water Fractions

[11] The water masses of the Arctic Ocean consist of a mixture of Atlantic Water, Pacific Water, river runoff, and sea ice melt/brine. The fractions of these that contribute to a specific sample can be computed from its chemical properties. In this contribution we are mainly interested in the fraction of sea ice brine, i.e., negative sea ice melt, and two approaches were applied, one for each of the data sets. For the Beringia data we applied the approach of *Jones et al.* [2008], where the Atlantic and Pacific contributions first were distinguished using the phosphate to nitrate relationship. Thereafter the fractions of freshwater sources were computed from salinity (S) and TA values by the equations

$$f^{AW} + f^{PW} + f^{si} + f^{r} = 1, \quad (2)$$

$$TA^{AW}f^{AW} + TA^{PW}f^{PW} + TA^{si}f^{si} + TA^{r}f^{r} = TA^{m}, \quad (3)$$

$$S^{AW}f^{AW} + S^{PW}f^{PW} + S^{si}f^{si} = S^{m}, \quad (4)$$

where the fractions of source water are denoted by f, and the indices AW, PW, si, r, and m stand for Atlantic Water, Pacific Water, sea ice, runoff and measured, respectively. The source water values assigned in the computations are given in Table 1. For a detailed description of the calculations we refer to *Jones et al.* [2008].

[12] Data from the Siberian shelf seas span a wide range of salinity as well as oxygen concentrations where the latter mainly is a result of mineralization of organic matter. Under these conditions total alkalinity behaves nonconservatively, making it less favorable to use in computing fresh water sources. Instead the $\delta^{18}O$ of the water can be used to determine the origin of the freshwater. There are detailed studies of the behavior of $\delta^{18}O$ in the Laptev and East Siberian Seas [*Bauch et al.*, 2011; *Persson et al.*, 2012]. Here we use the following equations:

$$f^{PW} + f^{si} + f^{r} = 1, \quad (5)$$

$$\delta^{18}O^{PW}f^{PW} + \delta^{18}O^{si}f^{si} + \delta^{18}O^{r}f^{r} = \delta^{18}O^{m}, \quad (6)$$

$$S^{PW}f^{PW} + S^{si}f^{si} = S^{m}, \quad (7)$$

where the Atlantic water was excluded because it makes only a minor contribution in the investigated area and will not impact the relation of freshwater sources. Because $\delta^{18}O$ varies in the different rivers, the value of the Kolyma river was applied (Table 1) because this flows into the East Siberian Sea where most samples were collected.

Table 1. Source Water Values Used to Compute the Fractions

	Salinity	$\delta^{18}O$ (‰)	TA (μmol/kg)
Sea ice, central Arctic Ocean	2.5		175[c]
Sea ice, Siberian shelf seas	4.0	2.8[a]	
Atlantic water	35	0.3[a]	2250[c]
Pacific water	32.7	–1.1[a]	2292[c]
Mean river runoff	0		1000[c]
Kolyma River annual mean water	0	–22.2[b]	

[a][*Ekwurzel et al.*, 2001].
[b][*Cooper et al.*, 2008].
[c][*Jones et al.*, 2008].

3. Results and Discussion

[13] In order to address the source and formation mechanisms of the Upper Halocline, one needs to identify its physical and chemical signature and distribution within the central basins. Then a description of the water mass properties on the Siberian shelf follows that leads to the conclusions.

3.1. The Central Basins

[14] The halocline layers of the central Arctic Ocean have a clear signature of brine from sea ice (negative sea ice melt) but with different depth distributions in the Eurasian and Canadian Basins (Figure 2). In the Amundsen and Makarov Basins the maximum brine contribution is found at about 50 m (Figure 2a) while in the Canada Basin it is spread over the range of 50–250 m (Figure 2b) depending on station position. A similar pattern in the brine distribution was found by *Yamamoto-Kawai et al.* [2005] in a thorough evaluation of the freshwater sources of the central Arctic Ocean using both TA and $\delta^{18}O$. The observed difference in the depth extent reflects the vertical salinity distribution of the basins, as is seen in a plot of fraction versus salinity (Figures 2c and 2d) where the maximum brine contribution is centered around a salinity of ~33 in both regions. However, the difference is that in the Canada Basin the maximum brine content is associated with a maximum in nutrients (here exemplified by silicate), which is not the case in the Amundsen and Makarov Basins (Figures 2e and 2f).

[15] The origin of the signature of the upper halocline, centered around a salinity of 33, was early on suggested to originate from sea ice brine produced over the continental shelves that mixes with underlying water to form a cold, saline water that is advected into the basins of the Arctic Ocean [*Aagaard et al.*, 1981; *Melling and Lewis*, 1982; *Cavalieri and Martin*, 1994]. This formation mechanism agrees with the high nutrient content observed is a result of organic matter mineralization at the sediment surface on the shelves with the decay products added to the cold, saline bottom water [e.g., *Kinney et al.*, 1970; *Jones and Anderson*, 1986; *Moore and Smith*, 1986].

[16] One question would be why the high nutrient content is confined to the Canada Basin and not found in the Amundsen and Makarov Basins during the 2005 Beringia cruise. Its extent has earlier been observed also in the

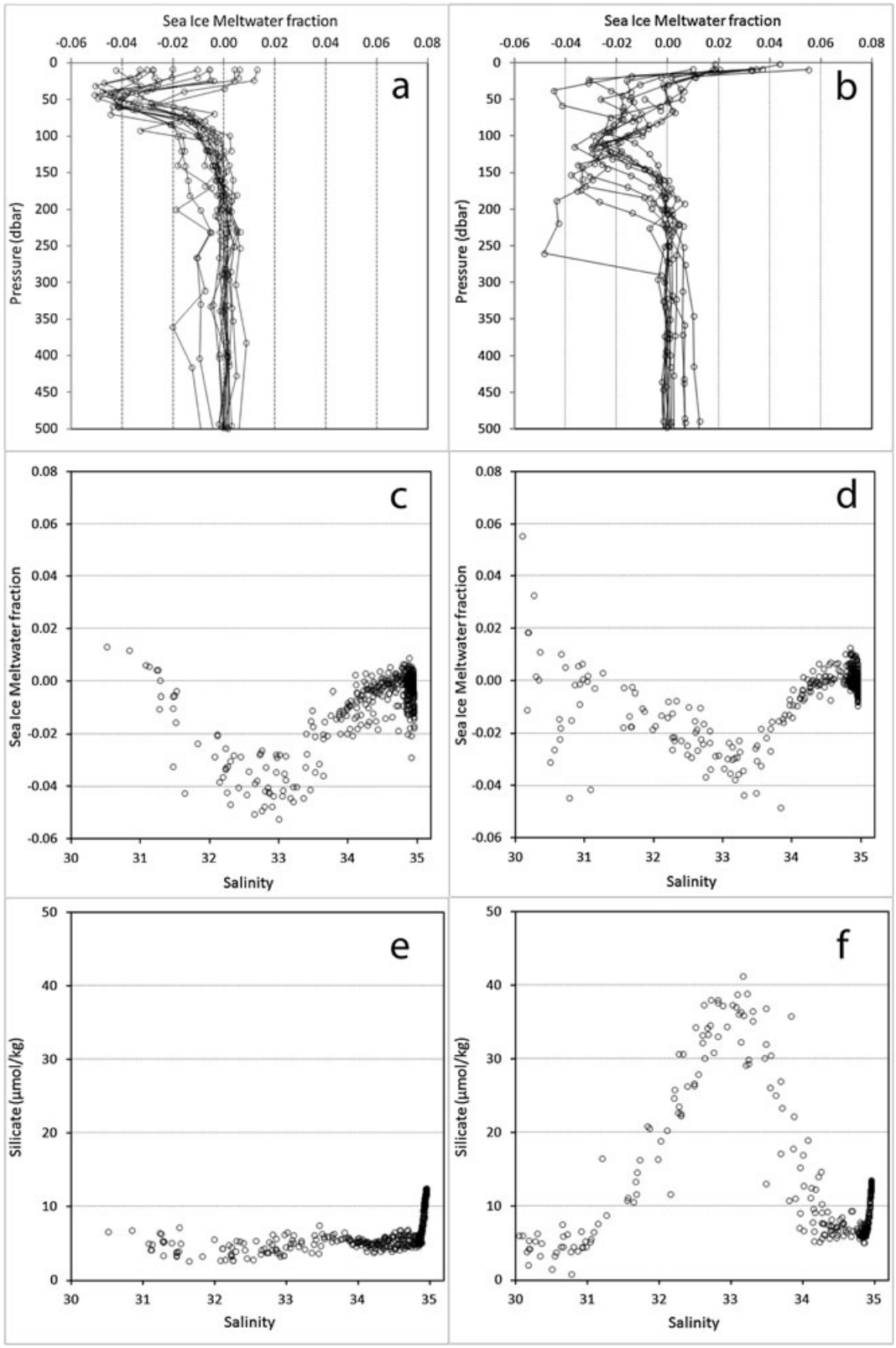

Figure 2. Distribution of sea ice melt water in the upper 500 m of (a) the Amundsen and Makarov Basins and (b) the Canada Basin, and as a function of salinity for the full depth in (c) the Amundsen and Makarov Basins and (d) the Canada Basin, as well as silicate concentration versus salinity for the full depth in (e) the Amundsen and Makarov Basins and (f) the Canada Basin.

Makarov Basin and as far over to the Atlantic side as the Lomonosov Ridge [e.g., *Moore et al*., 1983]. Consequently the extension of the nutrient maximum varies with time and is likely determined by the Beaufort Gyre that can vary in magnitude depending on the atmospheric pressure pattern [e.g., *Proshutinsky et al*., 2002; *Proshutinsky et al*., 2009]. The reason why the waters in the Atlantic sector do not contain this high nutrient water is due to the much lower nutrient concentrations in the inflowing Atlantic water in combination with little or no outflow of high nutrient brine-enriched water from the Barents and Kara Seas. The Barents Sea has high productivity [*Sakshaug*, 2004] but it is relatively deep (~200 m), resulting in less organic matter entering the sediment compared to the shallow Chukchi and East Siberian seas on the Pacific side of the Arctic Ocean. High-salinity brine-enriched waters have been observed in the eastern Barents Sea [*Midttun*, 1985], but no observation of a nutrient-rich water flowing out to the Arctic Ocean through the St. Anna Trough has been reported. However, these areas have been sparsely sampled and the details of this outflow are still open for speculation.

[17] That the water in the approximate upper 100 m in the Eurasian Basin has a brine signature, but no elevated nutrients, is likely a result of local sea ice formation. *Rudels et al*. [1996] suggest winter homogenization of the upper ~100 m by brine addition from sea ice formation within the Eurasian Basin. In our summer observation the surface water ($S < \sim 32$) is impacted by sea ice melt water giving a lower brine fraction close to the surface and the sea ice melt fraction profile has a minimum at about 50 m (Figure 2a).

3.2. The East Siberian and Western Chukchi Seas

[18] High primary production together with elevated concentrations of nutrients in bottom waters have been reported from the East Siberian and Laptev seas [e.g., *Codispoti and Richards*, 1968; *Olsson and Anderson*, 1997] and the Chukchi Sea [e.g., *Walsh et al*., 1989; *Cota et al*., 1996; *Codispoti et al*., 2005; *Lepore et al*., 2007]. The data collected in 2008 reveal that the high nutrient concentrations are associated with brine enrichment with generally increasing levels toward the bottom in both the East Siberian Sea and the Herald Valley in the Chukchi Sea (Figure 3). In Figure 3 the nutrients are represented by silicate with a similar pattern also seen for phosphate and nitrate. The elevated nutrient concentrations are coupled to a decrease in oxygen concentration and pH values, strongly supporting mineralization of organic matter as the process behind these signatures.

[19] The minimum oxygen concentration observed was close to 100 µmol/kg but nevertheless there was a substantial deficit in nitrate relative to phosphate as expressed by N^{**} values as low as –25. N^{**} equals $0.87[NO_3] - 16[\cdot PO_4] + 2.9$, which is a signature of loss in nitrate as a result of denitrification and/or anammox. One possible explanation for these low values could be that ammonium is formed during mineralization

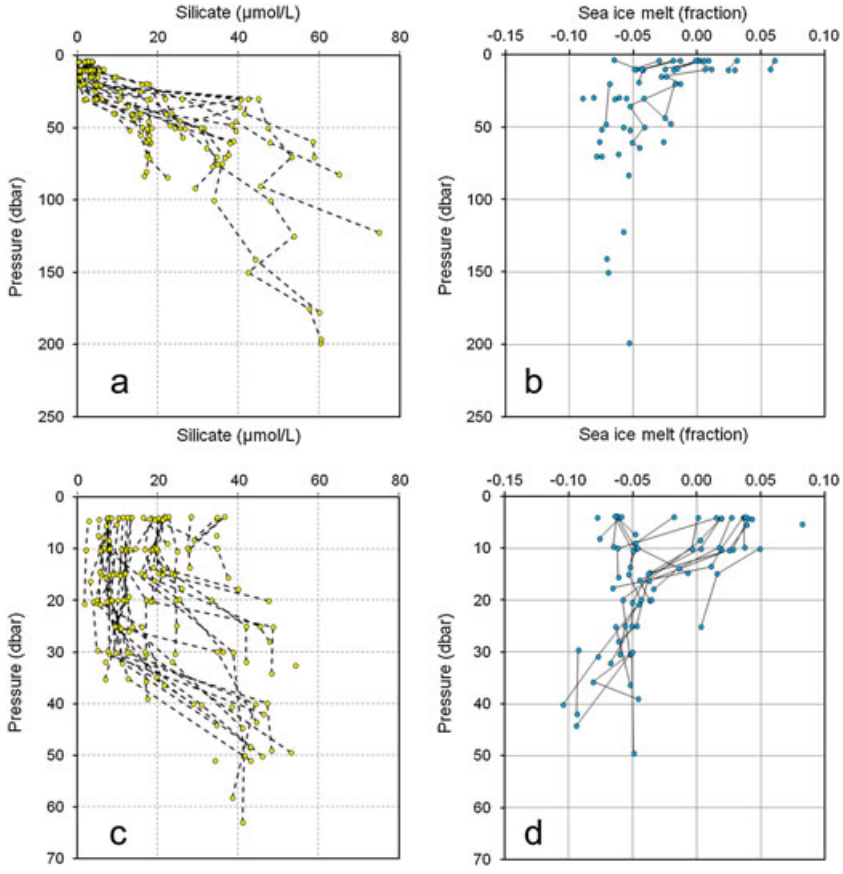

Figure 3. Silicate and sea ice melt fraction profiles from (a and b) the Herald Valley and (c and d) the East Siberian Sea.

but has not yet oxidized to nitrate. Ammonium was determined for some samples, including those of low N^{**}, but adding ammonium to the N^{**} expression only had a minor effect. Hence, it is likely that mineralization occurred at oxygen concentrations significantly lower than those observed in the water column. Such conditions are likely to be found in the surface sediments, making them a plausible environment for mineralization.

[20] That the mineralization signature is strongest close to the bottom and linked to brine enrichment lends further support to the hypothesis that mineralization occurs in surface sediments with the decay products released to the bottom water. This bottom water has had its salinity increased by addition of brine from sea ice formation, which was also observed in some waters with salinities < 30, close to the coast in the East Siberian Sea. This low-salinity, brine-enriched water was not observed in the outer parts of the shelf or the shelf slope, at least not with the same chemical signature. Hence, the waters of the shallow inner shelf are most likely mixed throughout the water column before exiting the East Siberian Sea.

3.3. The East Siberian Shelf Break

[21] High nutrient concentrations are found at the East Siberian shelf break in the depth range of 50 to 200 m (Figure 4). This nutrient-rich water also includes ~5% of brine, but unfortunately only a few samples for $\delta^{18}O$ were collected and no detailed profile is available. However, it is obvious that the surface water does not include brine, but rather a sea ice melt signal. Also, the deepest sample collected, > 1000 m, has a sea ice fraction of about zero. This is expected because it is of Atlantic water origin. Considering that the boundary current along this shelf break comes dominantly from the west [*Woodgate et al*., 2001] these data strongly suggest that nutrient-rich water is leaving the East Siberian Sea to contribute to the central Arctic Ocean halocline.

[22] A closer inspection of the salinity-nutrient property of this nutrient-rich water (Figure 5) reveal that high silicate concentrations are found in a larger salinity range (Si concentrations >30 µmol/L between 32.5 and 34.5 salinities) compared to past observations in the central Arctic Ocean, but similar to what *Nishino et al*. [2009] observed in 2004 in the same region. *Nishino et al*. [2009] had a higher vertical

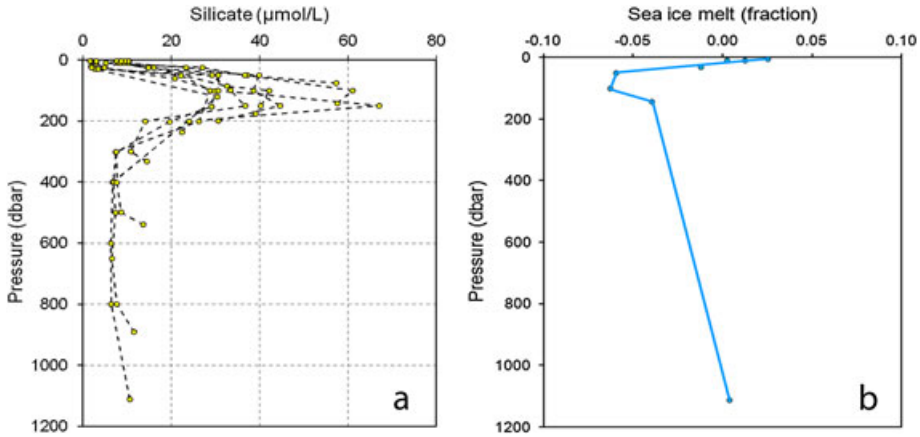

Figure 4. Profiles at the continental margin of the East Siberian Sea of silicate concentration (left) and sea ice melt water fraction (right) computed from $\delta^{18}O$ and salinity. Station locations are shown in Figure 1 right.

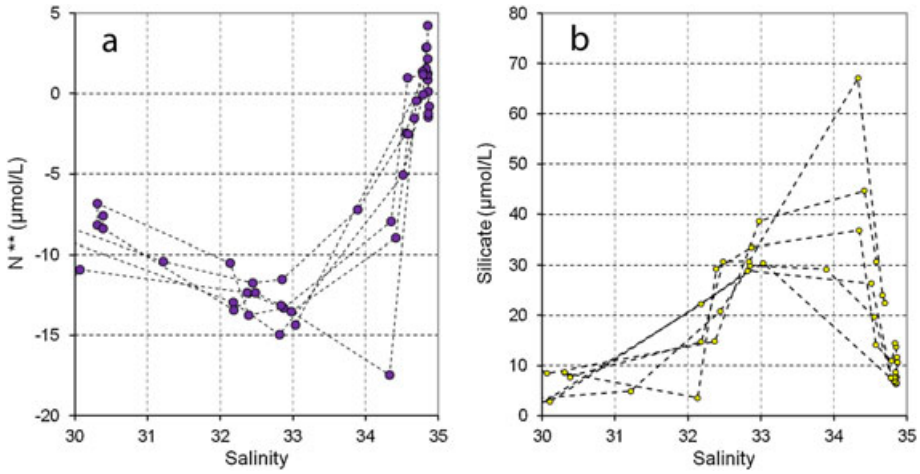

Figure 5. Silicate and N^{**} (=0.87[NO3] – 16[·PO4] + 2.9) versus salinity at the East Siberian Sea shelf slope.

sampling resolution and observed silicate maxima at $S \approx 32.5$ and at $S \approx 34$ relative to the concentration found in between these salinities and a minimum in N^{**} at $S \approx 32.5$. The 2008 data show minima of N^{**} at salinities between 32 and 33 depending on station, except for one sample with a minimum at higher salinity (Figure 5). This data point with the lowest N^{**} and highest silicate concentration also has the lowest oxygen concentration and lowest pH value. Hence, it is consistent with extensive mineralization, likely also in low oxygen environment, but because salinity was not determined directly on the water collected we cannot be sure that the CTD salinity reading is matching that of the water sample.

[23] A closer inspection of the silicate concentration and pH levels along a depth section from the Indigirka river estuary to the shelf slope (Figure 6) reveals that the data point with the maximum silicate concentration at a depth of about 150, close to the bottom, is accompanied by high concentrations at the same depth but farther off shore. The same goes for other constituents, like the pH minimum, which supports that the data close to the bottom at this depth has a signature of organic matter mineralization.

[24] From the section it is seen that bottom water all the way across the shelf and inshore of the 100 m isobath has high silicate and low pH values, although salinities >33 are only found at the shelf break. Hence, high-nutrient water with salinities > 33 has either left the shelf earlier in the season or it has left the shelf farther to the west. Alternatively it could have achieved its signature at the shelf break, but this is less likely because the negative N^{**} for salinities up to ~34.5 (Figure 5) suggest NO_3^- as electron acceptor, i.e., mineralization at low oxygen concentrations. Low oxygen concentrations are more likely to be produced close to the sediment surface on the shelf than along the continental margin, where a boundary current exists that supplies highly oxygenated water from the Atlantic. This argues against the suggestion by *Nishino et al*. [2009] that the silicate maximum at the high salinity (> 34) was produced by decomposition of opal-shelled organisms along the continental margin. Furthermore, all waters with silicate concentrations above 25 µmol/L found during the ISSS-08 expedition had a brine content of 4% or more (Figure 7). The brine signature is formed at the surface and in order to keep this signature it has to reach the bottom before being diluted by mixing with surrounding waters. Hence, it is not realistic that this water has reached its depth, ~150 m, without following the bottom from shallower regions of the shelf. Consequently it is unlikely that water of Atlantic origin is the source without modification on the shelf.

[25] Looking at the five stations located at the shelf break (bottom depth between 143 and 334 m) gives some more insight. An Θ-S plot (Figure 8) shows a distinct temperature minimum between a salinity of 32 and 33, surrounded by

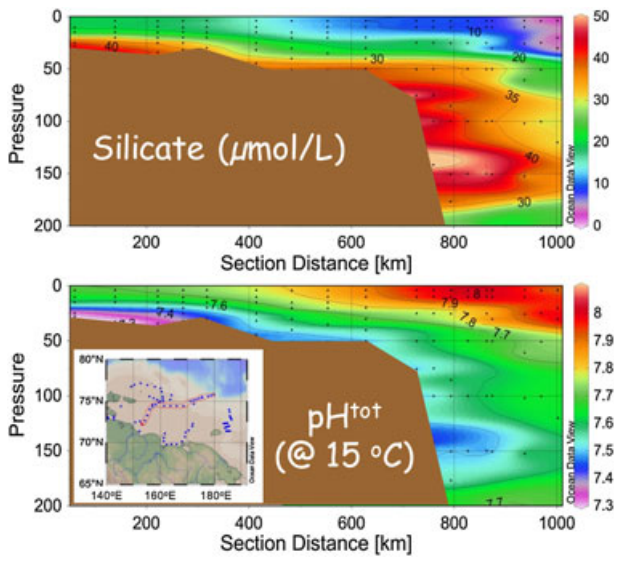

Figure 6. Depth sections of silicate and pH^{tot} along a section from the Indigirka River estuary to the shelf slope; see insert for station locations. The stippled line in the silicate section illustrates salinity 33 and the thick solid line salinity 34. Figure drawn by Ocean Data View [*Schlitzer*, 2011].

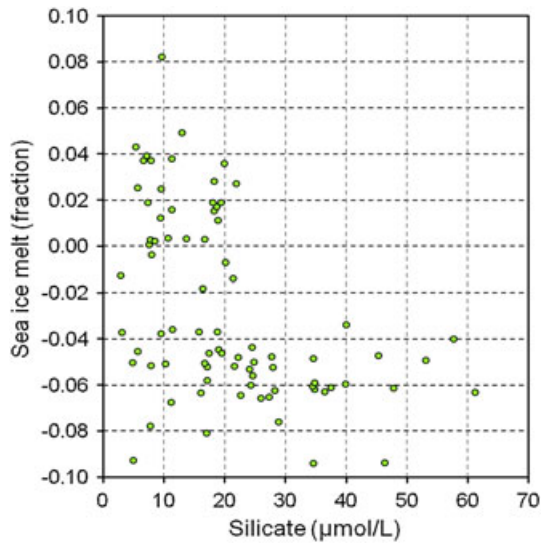

Figure 7. Sea ice melt fraction versus silicate concentration in the East Siberian Sea and shelf slope.

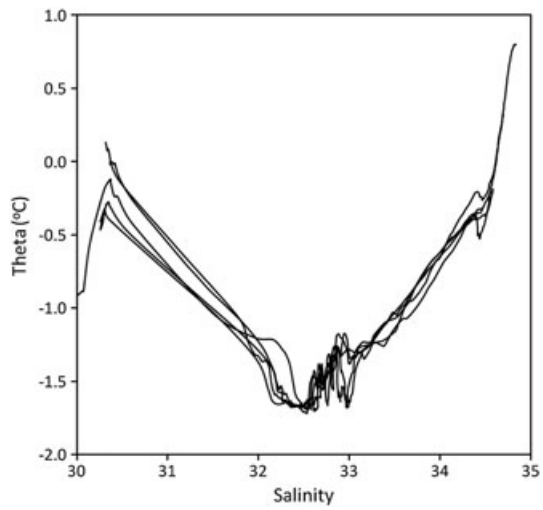

Figure 8. Temperature versus salinity for five stations at the East Siberian Sea shelf break, bottom depths between 143 and 334 m.

fairly linear mixing both toward lower and higher salinities. At a salinity of about 34.5, corresponding to a depth of about 150 m, there was a local temperature minimum indicating interleaving of a colder water mass. This water coincides with the deep, high salinity, silicate maximum (Figure 9d), and could give an indication of the source of this maximum. *Nishino et al*. [2009] did not observe such a distinct T minimum at this salinity, but there was a clear bend in their T-S diagram. This difference is likely a result of their stations being positioned farther away from the shelf break where mixing would smooth these details. The outermost station during the ISSS-08 cruise showed the same smooth Θ-S curve as reported in *Nishino et al*. [2009].

[26] In the depth range 50–100 m temperatures were close to freezing, salinities were between about 32.5 and 33.5 and the oxygen concentrations were around 300 µmol/kg, except for a few samples where the concentration was substantially lower (Figures 9a–9c). The silicate concentrations were elevated and the pH^{tot} as well as N^{**} values were lower compared to the surface water (Figures 9d–9f). The low pH^{tot} is a sign of mineralization of organic matter, and the low N^{**} is a sign of mineralization at suboxic conditions. However, the measured oxygen concentrations of about 300 µmol/kg in the water column demonstrates that the anoxic conditions must prevail in the sediments where the mineralization occurs and the decay products are released to the bottom water.

[27] At depths around 150 m on the shelf slope the oxygen concentrations and pH^{tot} values have minima, and the silicate concentrations are high, clearly showing that mineralization of organic matter is important for the properties of these waters. However, the N^{**} values are about the mean of the minimum values and those found at 300 m depth, and the same is true for temperature. Hence, assuming that the source water was at a freezing temperature (suggested by brine being present, Figure 7) the water at 150 m depth could be a one-to-one mixture of the source water and the water at 300 m depth. Such a mixture would give source water concentrations of oxygen between 0 and 100 µmol/kg, silicate between 70 and 110 µmol/L, pH^{tot} between 7.0 and 7.4 and salinity ≈ 34.0. For oxygen, silicate and pH^{tot} this is about what has been observed as extreme values on the shelf, making this a plausible mixing scenario. The same is true for phosphate and nitrate, where the source water concentrations would be about 2.2 and 18 µmol/L, respectively.

[28] The halocline water at the slope section likely flows to the east in a similar pattern as the lower halocline and Atlantic Layer water does at the Laptev Sea [*Dmitrenko et al*., 2011, and references therein]. Considering that the high-nutrient and low-pH waters show the strongest signal close to the continental slope (Figure 6) it is unlikely that these waters have their source in any other region than between the Laptev Sea and the observation region. Furthermore, because no water with silicate levels above 10 µmol/kg was found at the shelf slope in the middle of the Laptev Sea during the summers of 2007 to 2009 [*Dmitrenko et al*., 2011] this will even limit the likely region of formation to the east of about 140°E. However, the question is if waters of the observed properties can be found anywhere on the shelf.

[29] The lowest oxygen and N^{**} concentrations and pH^{tot} values observed on the shelf were around a position of 73°N and 155°E (Figure 10), making this region a plausible source

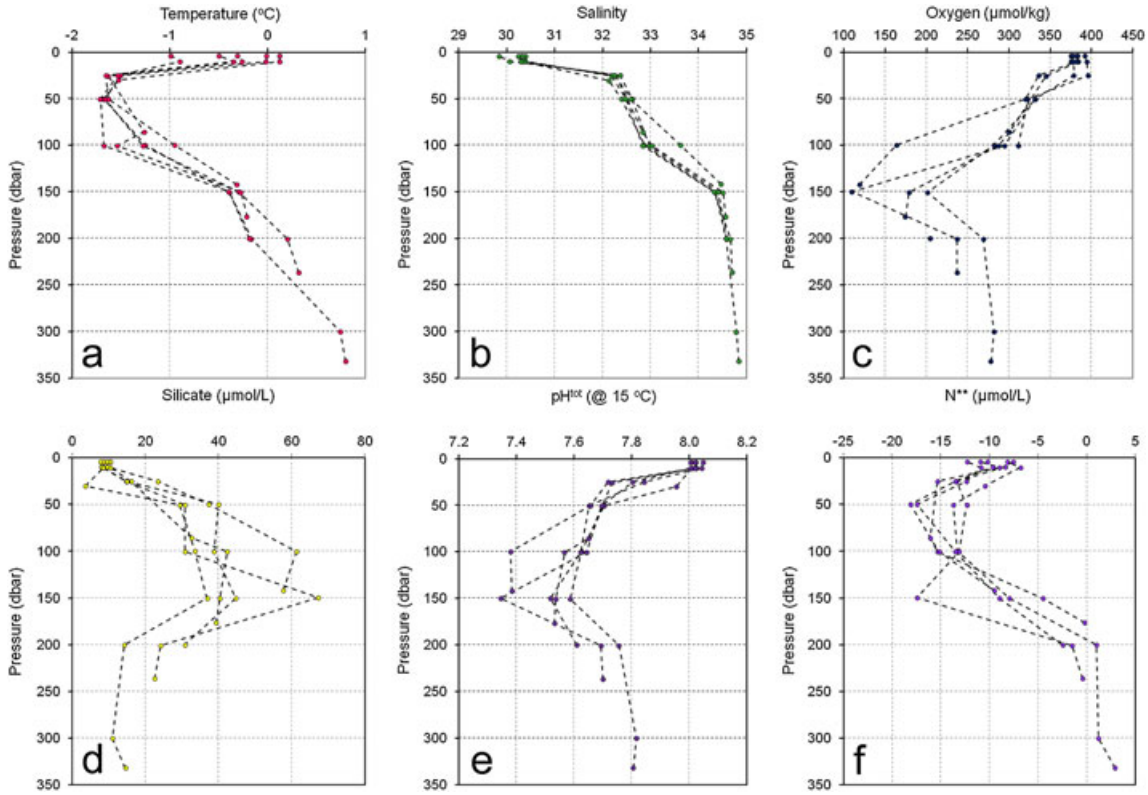

Figure 9. Profiles of (a) temperature, (b) salinity, (c) oxygen, (d) silicate, (e) pH^{tot}(15°C), and (f) N^{**}, for the same five stations as in Figure 8.

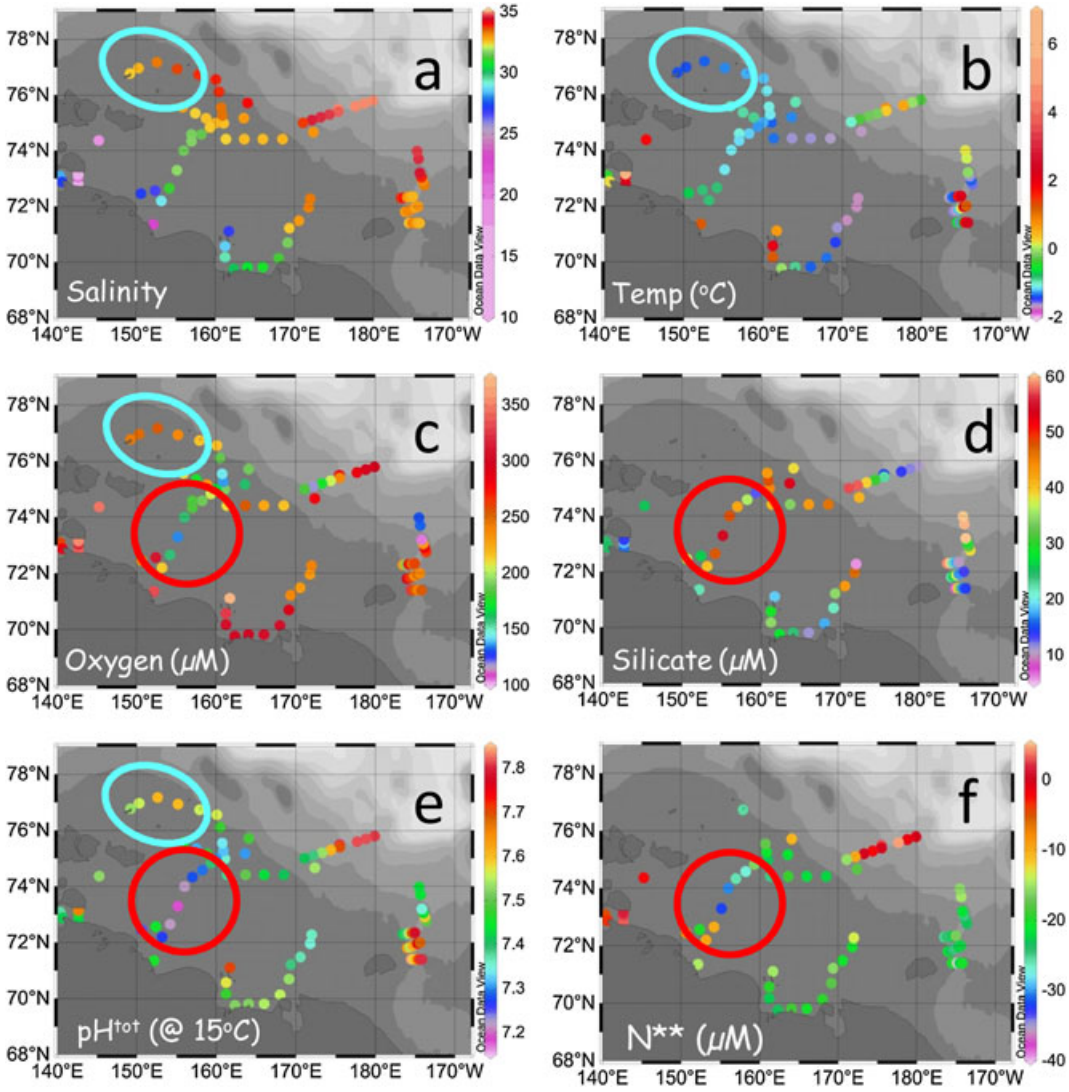

Figure 10. Bottom water properties of (a) salinity, (b) temperature, (c) oxygen, (d) silicate, (e) pH^{tot} (at 17°C), and (f) *N*** in the East Siberian Sea and the western Laptev Sea. The red circle shows the region with biogeochemical signature of active mineralization of organic matter, while the blue circle shows the region with cold water of relatively high salinity and signature of some mineralization of organic matter. Figure drawn by Ocean Data View [*Schlitzer*, 2011].

area for the *N*** minimum found at 50–100 m depth at the shelf break. At this site the salinities were lower than observed at the shelf break, ~31.5 compared to 32.5, and the temperatures were higher, –1.1 °C compared to –1.7 °C. This study was performed in mid-September, opening for substantial mixing after the ice breakup in June-July.

[30] For the deep silicate maximum even higher salinities are observed. Using idealized models *Dethleff* [2010] computed volume and salinities of brine-induced shelf plumes in the flaw leads of the Laptev Sea. In the region north of the New Siberian Islands the computed production of water with salinities above 34 was more than 0.02 Sv, with about 80% of this production occurring in the winter and 20% in the fall. This is the region where the surface water is least impacted by the runoff from mainly the Lena River and thus also the region where the highest salinities are likely to be found. The ISSS-08 cruise covered a part of the region north of the New Siberian Islands and the bottom water had salinities over 33, temperatures down to –1.3 °C, pH^{tot} (at 15 °C) under 7.6, and oxygen under 250 μmol/kg (Figure 10). Unfortunately, no nutrient data were available. The observations are not within the range of the required source water properties, but they were done in mid-September about half a year after the peak of winter conditions. Hence, there were ample time for the dense waters to leave the shelf and also an ice-free summer likely contributed to efficient mixing in these shallow waters of 35 to 65 m depth. Nevertheless, both oxygen and pH^{tot} decreased from the surface to the bottom, pointing to a clear signature of mineralization of organic matter.

[31] From the few existing observations of brine-enriched dense shelf waters formed by polynyas it can be assumed that the high salinity bottom water layer formed outside the actual polynya area is rather thin. Observations in the Chukchi Sea [*Aagaard et al.*, 1981] indicate a layer thickness of less than 5 m. The strong vertical salinity stratification in such layer would also suppress the vertical mixing. This

can increase the concentration of the decay products in the water above the sediments compared to the summer situation if the decay rate is similar. Mooring observations outside the New Siberian Islands at the 1700 m isobaths [*Woodgate et al*. 2001] show mean currents between 2.0–2.7 cm s^{-1} in the upper 300 m and it is likely that the speed is somewhat higher further up the slope. Using an advection speed of 5 cm/s and the distance between the New Siberian Islands and the shelf slope section of 650 km gives an advective time scale of around 6 months. This fits well with the hypothesis that the water observed at the slope has been formed at this shelf region during the previous winter.

4. Summary and Conclusions

[32] The surface waters of the central Arctic Ocean with salinities between about 32 and 34, i.e., the halocline, have a signature of brine from sea ice formation. Waters with lower salinity observed in the summer have a signature of less brine or even of sea ice melt water. However, in the region influenced by Pacific water there is also a distinct nutrient maximum within this salinity range, a signature of organic matter mineralization on the adjacent shelves. The exact distribution of the nutrient maximum within the central Arctic Ocean has varied in time and has been suggested to depend on the dominating atmospheric pressure field.

[33] Summer observations from the East Siberian Sea and Herald Valley in the Chukchi Sea reveal that the majority of waters below 10 m depth have a strong signature of sea ice brine. Most of these waters also have elevated nutrient concentrations and low oxygen and pH, illustrating the mineralization of organic matter. A deficit in nitrate relative to phosphate, a signature of denitrification or anammox, indicates that much of this mineralization occurs at lower oxygen concentrations than those observed in the water column. The most plausible explanation is mineralization at the sediment surface with the decay products leaking back to the bottom water, a bottom water enriched in salinity from sea ice brine. A similar signature in salinity, brine properties as well as other chemical constituents was also observed at the East Siberian shelf break, illustrating the contribution to the UH from this area of the Arctic shelves.

[34] The observed excess of nutrients at the shelf break, exemplified by silicate, covered an interval including higher salinities in 2008 compared to the observations in 2005 in the central Canada Basin. The high-silicate, high-salinity water was also observed in 2004 north of the East Siberian Sea [*Nishino et al*., 2009]. Because our study was performed during summer no direct observations of high-silicate, high-salinity water was observed on the shelf, but from the knowledge of the eastward flow along the continental slope it is highly likely that the formation area is west of our observation area. One way to change the marine environment is a change in seasonal sea ice coverage and indeed less summer sea ice cover has been observed over the East Siberian Sea during the last decades, especially since 2001 (Figure 11). We hypothesize that this has resulted in more brine production by sea ice formation, all the way from the coast out to the shelf break. In the outer parts of the shelf, e.g., north of the East Siberian Islands, the resulting bottom water thus could obtain a higher salinity like the observed increase in the salinity of the high silicate water. Consequently this results in different

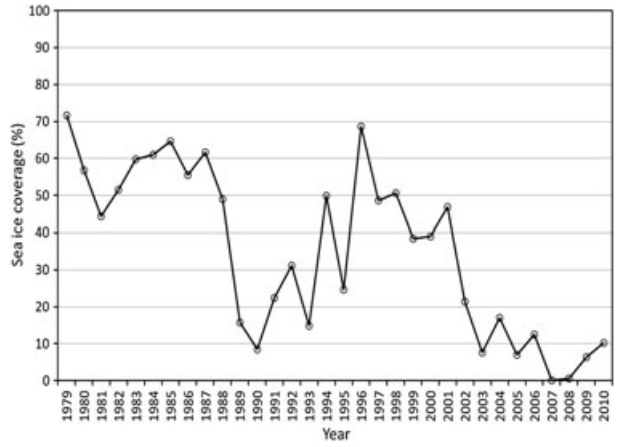

Figure 11. Sea ice coverage in the East Siberian Sea during the month of September as evaluated from the passive microwave data of National Snow and Ice Data center (NSIDC) [*Cavalieri et al*., 1996]. Data are from the region: latitude 70°N to 77.5°N, longitude 145°E to 180°E.

regions for production of nutrient-rich halocline waters, for instance one in the midshelf where waters of salinity of 32–33 is produced and one at the outer shelf where nutrient-rich water of salinity around 34 is produced. Waters from both sources would flow out to the continental break where they interleave at their appropriate density surface while flowing toward the east (Figure 12). This is at present only a hypothesis that present one of a few plausible explanations to the observed water property signatures. Future studies will show if our hypothesis are correct and if the nutrient-rich high-salinity water found at the shelf break also will spread into the central basins and possibly lead to an expansion to a large depth range. Whatever the location of formation areas are our observations show that there must be at least two different formation areas in the East Siberian Sea for the nutrient-rich halocline of the central Arctic Ocean. This is in addition to the formation areas of the Chukchi Sea, where we also identified the Herald Valley as one important route.

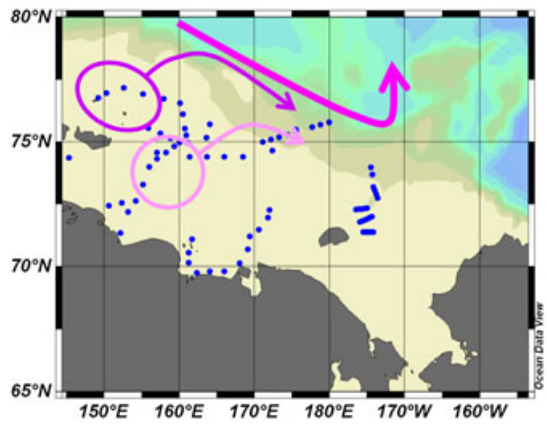

Figure 12. Hypothetical formation of the halocline properties found at the East Siberian shelf break. Figure based on drawing by Ocean Data View [*Schlitzer*, 2011].

[35] **Acknowledgments.** Financial support was received from the Knut and Alice Wallenberg Foundation, the Swedish Research Council (contract 621-2010-4084), the European Union FP7 projects EPOCA (contract 211384) and CarboChange (under grant 264879). We would like to thank Tom Weingartner for constructive comments on an earlier version of this manuscript.

References

Aagaard, K., L. K. Coachman, and E. C. Carmack (1981), On the halocline of the Arctic Ocean, *Deep-Sea Res., A 28*, 529–545.

Anderson, L. G., G. Björk, O. Holby, G. Kattner, P. K. Koltermann, E. P. Jones, B. Liljeblad, R. Lindegren, B. Rudels, and J. Swift (1994), Water Masses and Circulation in the Eurasian Basin: Results from the Oden 91 North Pole Expedition, *J. Geophys. Res.*, *99*, 3273–3283.

Anderson, L. G., T. Tanhua, G. Björk, S. Hjalmarsson, E. P. Jones, S. Jutterström, B. Rudels, J. H. Swift, I. Wåhlström (2010), Arctic Ocean shelf – basin interaction, an active continental shelf CO_2 pump and its impact on the degree of calcium carbonate dissolution, *Deep Sea Res., I 57*, 869–879 doi:10.1016/j.dsr.2010.03.012.

Arrigo, K. R., G. van Dijken, and S. Pabi (2008), Impact of a shrinking Arctic ice cover on marine primary production, *Geophys. Res. Lett.*, *35*, L19603, doi:10.1029/2008GL035028.

Bauch D., M. Rutgers van der Loeff, N. Andersen, S. Torres-Valdes, K. Bakker, and E. P. Abrahamsen (2011), Origin of freshwater and polynya water in the Arctic Ocean halocline in summer 2007, *Prog. Ocean.*, *91*, 482–495.

Cavalieri, J. D., and S. Martin (1994), The contribution of Alaskan, Siberian and Canadian coastal polynyas to the cold halocline layer of the Arctic Ocean, *J. Geophys. Res. 99*, 18343–18362.

Cavalieri, D., C. Parkinson, P. Gloersen, and H. J. Zwally (1996, updated yearly.), Sea Ice Concentrations from Nimbus-7 SMMR and DMSP SSM/I-SSMIS Passive Microwave Data, [1996-01-01; 2010-12-31]. Boulder, Colorado USA: National Snow and Ice Data Center. Digital media.

Clayton, T. D., and R. H. Byrne (1993), Spectrophotometric seawater pH measurements: total hydrogen ion concentration scale calibration of m-cresol purple and at-sea results, *Deep-Sea Res. Part I*, *40*, 2115–2129.

Codispoti, L. A., and F. A. Richards (1968), Micronutrient distributions in the East Siberian and Laptev seas during summer 1963, *Arctic*, *21*, 67–83.

Codispoti, L. A., C. Flagg, V. Kelly, and J. H. Swift (2005), Hydrographic conditions during the 2002 SBI process experiments, *Deep-Sea Res. Part II*, *52*, 3199–3226, doi: 10.1016/j.dsr2.2005.10.007.

Cooper, L. W., J. W. McClelland, R. M. Holmes, P. A. Raymond, J. J. Gibson, C. K. Guay, and B. J. Peterson (2008), Flow-weighted values of runoff tracers (d18O, DOC, Ba, alkalinity) from the six largest Arctic rivers, *Geophys. Res. Lett.*, *35*, L18606, doi:10.1029/2008GL035007.

Cota, G. F., L. R. Pomeroy, W. G. Harrison, E. P. Jones, F. Peters, W. M. Sheldon Jr., and T. R. Weingartner (1996), Nutrients, primary production and microbial heterotrophy in the south eastern Chukchi Sea: Arctic summer nutrient depletion and heterotrophy, *Mar. Ecol., Prog. Ser. 135*, 247–258.

Dethleff, D. (2010), Dense water formation in the Laptev Sea flaw lead, *J. Geophys. Res.*, *115*, C12022, doi:10.1029/2009JC006080.

Dmitrenko, I. A., V. V. Ivanov, S. A. Kirillov, E. L. Vinogradova, S. Torres-Valdes, and D. Bauch (2011), Properties of the Atlantic derived halocline waters over the Laptev Sea continental margin: Evidence from 2002 to 2009, *J. Geophys. Res.*, *116*, C10024, doi:10.1029/2011JC007269.

Ekwurzel, B., P. Schlosser, R. A. Mortlock, and R. G. Fairbenks (2001), River runoff, sea ice meltwater, and Pacific water distribution and mean residence times in the Arctic Ocean, *J. Geophys. Res.*, *106*, C5, 9075–9092.

Gordon, L. I., J. C. Jennings, A. A. Ross, and J. M. Krest (1993), A suggested protocol for continuous flow automated analysis of seawater nutrients (phosphate, nitrate, nitrite and silicic acid) in the WOCE Hydrographic Program and the Joint Global Ocean Fluxes Study, WOCE Hydrographic Program Office, Methods Manual WHPO 91-1. (Available at http://whpo.ucsd.edu/manuals/pdf/91_1/gordnut.pdf)

Haraldsson C., L. G. Anderson, M. Hassellöv, S. Hulth, and K. Olsson (1997), Rapid, high-precision potentiometric titration of alkalinity in the ocean and sediment pore waters, *Deep-Sea Res. I 44*, 2031–2044.

Houssais, M.-N., C. Herbaut, P. Schlichtholz, and C. Rousset (2007), Arctic salinity anomalies and their link to the North Atlantic during a positive phase of the Arctic Oscillation, *Prog. Ocean.*, *73*, 160–189.

Jahn, A., B. Tremblay, L. A. Mysak, and R. Newton (2010), Effect of the large-scale atmospheric circulation on the variability of the Arctic Ocean freshwater export, *Clim. Dyn. 34*, 201–222, doi:10.1007/s00382-009-0558-z.

Johnson, K. M., J. M. Sieburth, P. J. Williams, and L. Brändström (1987), Coulometric total carbon dioxide analysis for marine studies: automation and calibration, *Mar. Chem. 21*, 117–133.

Jones, E. P., and L. G. Anderson (1986), On the Origin of the Chemical Properties of the Arctic Ocean Halocline, *J. Geophys. Res. 91*, 10759–10767.

Jones E. P., L. G. Anderson, S. Jutterström, and J. H. Swift (2008), Sources and Distribution of Fresh water in the East Greenland Current, *Prog. Ocean.*, *78*, 37–44, doi:10.1016/j.pocean.2007.06.003.

Kinney, P., M. E. Arhelger, D. Burrell (1970), Chemical characteristics of water masses in the Amundsen Basin of the Arctic Ocean, *J. Geophys. Res. 75*, 4097–4104.

Lee, K., and F. J. Millero (1995), Thermodynamic studies of the carbonate system in seawater, *Deep-Sea Res., I*, *42*, 2035–2061.

Lepore, K., S. B. Moran, J. M. Grebmeier, L. M. Cooper, C. Lalande, W. Maslowski, V. Hill, N. R. Bates, D. A. Hansell, J. T. Mathis, and R. P. Kelly (2007), Seasonal and interannual changes in particulate organic carbon export and deposition in the Chukchi Sea, *J. Geophys. Res. 112*, C10024, doi:10.1029/2006JC003555.

McPhee, M. G., A. Proshutinsky, J. H. Morison, M. Steele, and M. B. Alkire (2009), Rapid change in freshwater content of the Arctic Ocean, *Geophys. Res. Lett. 36*, doi:10.1029/2009GL037525.

Melling, H., and E. L. Lewis (1982), Shelf drainage flows in the Beaufort Sea and their effect on the Arctic Ocean pycnocline, *Deep-See Res.*, *29*, 967–985.

Midttun, L. (1985), Formation of dense bottom water in the Barents Sea, *Deep-Sea Res.*, *32*, 1233–1241.

Moore, R. M., and J. N. Smith (1986), Disequilibria between ^{226}Ra, ^{210}Pb and ^{210}Po in the Arctic Ocean and the implication of chemical modification of the Pacific water inflow, *Earth Planet. Sci, Lett.*, *77*, 285–292.

Moore, R. M., M. G. Lowings, and F. C. Tan (1983), Geochemical profiles in the Central Arctic Ocean: Their relation to freezing and shallow circulation, *J. Geophys. Res.*, *88*, 2667–2674.

Nishino, S, K. Shimada, M. Itoh, and S. Chiba (2009), Vertical Double Silicate Maxima in the Sea-Ice Reduction Region of the Western Arctic Ocean: Implications for an Enhanced Biological Pump due to Sea-Ice Reduction *J. Oceanogr*, *65*, 871–883.

Olsson, K., and L. G. Anderson (1997), Input and biogeochemical transformation of dissolved carbon in the Siberian shelf seas, *Cont. Shelf Res.*, *17*, 819–833.

Pabi, S., G. L. van Dijken, and K. R. Arrigo (2008), Primary production in the Arctic Ocean, 1998–2006, *J. Geophys. Res. 113*, C08005, doi:10.1029/2007JC004578.

Persson P-O., P. S. Andersson, D. Porcelli, V. Alling, G. Björk, and C.-M. Mörth (2012), Ice export from Laptev and East Siberia Sea derived from δ^{18}O, manuscript.

Proshutinsky, A., R. H. Bourke, and F. A. McLaughlin (2002), The role of the Beaufort Gyre in Arctic climate variability: Seasonal to decadal climate scales, *Geophys. Res. Lett.*, *29*(23), 2100, doi:10.1029/2002GL015847.

Proshutinsky, A., R. Krishfield, M.-L. Timmermans, J. Toole, E. Carmack, F. McLaughlin, W. J. Williams, S. Zimmermann, M. Itoh, and K. Shimada (2009), Beaufort Gyre freshwater reservoir: State and variability from observations, *J. Geophys. Res.*, *114*, C00A10, doi:10.1029/2008JC005104.

Rudels, B., L. G. Anderson, and E. P. Jones (1996), Formation and evolution of the surface mixed layer and halocline of the Arctic Ocean, *J. Geophys. Res.*, *101*, 8807–8821.

Rudels, B., E. P. Jones, L. G. Anderson and G. Kattner (1994), On the intermediate depth waters of the Arctic Ocean, in The Polar Oceans and Their Role in Shaping the Global Environment, edited by O. M. Johannessen R.D. Muench and J.E. Overland, American Geophysical Union, Washington, D.C., 33–46.

Sakshaug, E. (2004), Primary and secondary production in the Arctic seas, in: The Organic Carbon Cycle in the Arctic Ocean, edited by: Stein, R. and Macdonald, R. W., Springer, New York, 57–81.

Schlitzer, R. (2011), Ocean Data View, http://odv.awi.de.

Schlosser, P., B. Kromer, B. Ekwurzel, G. Bönisch, A. McNichol, R. Schneider, K. von Reden, H. G. Östlund, and J. H. Swift (1997), The first trans-Arctic 14C section: comparison of the mean ages of the deep waters in the Eurasian and Canadian basins of the Arctic Ocean, *Nucl. Instr. Methods Physics Res., B*, *123*, 431–437.

Serreze, M. C., A. P. Barrett, A. G. Slater, R. A. Woodgate, K. Aagaard, R. B. Lammers, M. Steele, R. Moritz, M. Meredith, and C. M. Lee (2006), The large-scale freshwater cycle of the Arctic, *J. Geophys. Res. 111*, doi:10.1029/2005JC003424.

Tanhua T., E. P. Jones, E. Jeansson, S. Jutterström, W. M. Smethie Jr., D. W. R. Wallace, L.G. Anderson (2009), Ventilation of the Arctic Ocean: mean ages and inventories of anthropogenic CO2 and CFC-11, *J. Geophys. Res.*, *114*, C01002, doi:10.1029/2008JC004868.

Timmermans, M.-L., A. Proshutinsky, R. A. Krishfield, D. K. Perovich, J. A. Richter-Menge, T. P. Stanton, and J. M. Toole (2011), Surface freshening in the Arctic Ocean's Eurasian Basin: An apparent consequence of recent change in the wind-driven circulation, *J. Geophys. Res.*, *116*, C00D03, doi:10.1029/2011JC006975.

Walsh, J. J., C. P. McRoy, L. K. Coachman, J. J. Goering, J. J., Nihoul, T. E. Whitledge, T. H. Blackburn, P. L. Parker, C. D. Wirick, P. G. Shuert, J. M. Grebmeier, A. M. Springer, R. D. Tripp, D. Hansell, S. Djenidi, E. Deelersnijder, K. Henriksen, B. A. Lund, P. Andersen, F. E. Müller-Karger, and K. Dean (1989), Carbon and nitrogen cycling within the Bering/Chukchi Seas: source regions for organic matter affecting AOU demands of the Arctic Ocean, *Prog. Oceanogr. 22*, 279– 361.

Woodgate R. A., K. Aaagard, R. D. Muench, J. Gunn, G. Björk, B. Rudels, A. T. Roach, and U. Schauer (2001), The Arctic Ocean boundary current along the Eurasian slope and the adjacent Lomonosov Ridge: Water mass properties, transports and transformation from moored instruments, *Deep Sea Res.*, *48*, 1757–1792.

Yamamoto-Kawai, M., N. Tanaka, and S. Pivovarov (2005), Freshwater and brine behaviors in the Arctic Ocean deduced from historical data of $\delta^{18}O$ and alkalinity (1929-2002 A.D.), *J. Geophys. Res. 110*, doi:10.1029/2004JC002793.

Yamamoto-Kawai, M., F. A. McLaughlin, and E. C. Carmack (2011), Effects of ocean acidification, warming and melting of sea ice on aragonite saturation of the Canada Basin surface water, *Geophys. Res. Lett.*, *38*, L03601, doi:10.1029/2010GL045501.